

AD-A271 695 INFORMATION PAGE

Form Approved

OMB No. 0704-0188



to average 1 hour per response, including the time for reviewing instructions, searching existing data sources, gathering the collection of information. Send comments regarding this burden estimate or any other aspect of this form to Washington Headquarters Services, Directorate for Information Operations and Reports, 1215 Jefferson Davis Highway, Suite 1204, Arlington, VA 22202-4302, and to the Office of Management and Budget, Paperwork Reduction Project (0704-0188), Washington, DC 20503.

Davis Highway, Suite 1204, Arlington, VA 22202-4302, and to the Office of Management and Budget, Paperwork Reduction Project (0704-0188), Washington, DC 20503

1. AGENCY USE ONLY (Leave blank)		2. REPORT DATE		3. REPORT TYPE AND DATES COVERED	
4. TITLE AND SUBTITLE The Conformation of Fluid Membranes: Monte Carlo Simulations				5. FUNDING NUMBERS DAAL03-89-C-0038 (2)	
6. AUTHOR(S) D. M. Kroll and G. Gompper					
7. PERFORMING ORGANIZATION NAME(S) AND ADDRESS(ES) University of Minnesota - School of Mathematics 127 Vincent Hall Minneapolis, MN 55455					
9. SPONSORING/MONITORING AGENCY NAME(S) AND ADDRESS(ES) U. S. Army Research Office P. O. Box 12211 Research Triangle Park, NC 27709-2211				10. SPONSORING/MONITORING AGENCY REPORT NUMBER AKO 27747.176-MA-COE	
11. SUPPLEMENTARY NOTES The view, opinions and/or findings contained in this report are those of the author(s) and should not be construed as an official Department of the Army position, policy, or decision, unless so designated by other documentation.					
12a. DISTRIBUTION/AVAILABILITY STATEMENT Approved for public release; distribution unlimited.				12b. DISTRIBUTION CODE	
13. ABSTRACT (Maximum 200 words) The conformation and scaling properties of self-avoiding fluid membranes with an extrinsic bending rigidity κ were studied with the use of Monte Carlo methods. For $\kappa = 0$, the results are consistent with branched polymer behavior at large length scales. There is a smooth crossover from a crumpled to an extended state with increasing κ , with a peak in the specific heat when the persistence length reaches the system size. The scale-dependent effective bending rigidity is a decreasing function of system size for all bare rigidities. These results indicate that fluid membranes are always crumpled at sufficiently long length scales.					
14. SUBJECT TERMS				15. NUMBER OF PAGES	
17. SECURITY CLASSIFICATION OF REPORT UNCLASSIFIED				16. PRICE CODE	
18. SECURITY CLASSIFICATION OF THIS PAGE UNCLASSIFIED		19. SECURITY CLASSIFICATION OF ABSTRACT UNCLASSIFIED		20. LIMITATION OF ABSTRACT UL	

93-24866



93 10 18166

**Best
Available
Copy**

The Conformation of Fluid Membranes: Monte Carlo Simulations

D. M. KROLL* AND G. GOMPPER

Accession For	
NTIS CRA&I	<input checked="checked" type="checkbox"/>
DTIC TAB	<input type="checkbox"/>
Unannounced	<input type="checkbox"/>
Justification	
By	
Distribution /	
Availability Codes	
Dist	Avail and/or Special
A-1	20

DTIC QUALITY INSPECTED

The Conformation of Fluid Membranes: Monte Carlo Simulations

D. M. KROLL* AND G. GOMPPER

The conformation and scaling properties of self-avoiding fluid membranes with an extrinsic bending rigidity κ were studied with the use of Monte Carlo methods. For $\kappa = 0$, the results are consistent with branched polymer behavior at large length scales. There is a smooth crossover from a crumpled to an extended state with increasing κ , with a peak in the specific heat when the persistence length reaches the system size. The scale-dependent effective bending rigidity is a decreasing function of system size for all bare rigidities. These results indicate that fluid membranes are always crumpled at sufficiently long length scales.

MEMBRANES COMPOSED OF AM-
phiphilic molecules, such as the
monolayers of surfactant mole-
cules at oil-water interfaces in microemul-
sions, the lipid bilayers that form biological
membranes, as well as the layers of surfac-
tant molecules in recently studied lyotropic

liquid crystals, are highly flexible (nearly
tensionless) surfaces. Membranes play a cen-
tral role in determining the architecture of
biological systems and provide the basic
structural element for complex fluids such as
microemulsions; an understanding of the
statistical mechanics of these self-avoiding
surfaces is therefore of considerable impor-
tance (1, 2).

In most cases of interest, these mem-
branes are fluid, which means that the mol-
ecules can diffuse rapidly within the mem-
brane surface and possess no reference
lattice. In the absence of a lateral tension (3,

4), the shape of the membrane is governed
by its bending rigidity κ . A membrane of
linear size L exhibits transverse fluctuations
(5) of extension $L_{\perp} \sim (kT/\kappa)^{1/2} L$ (where k
is Boltzmann's constant and T is tempera-
ture) on length scales small compared to the
persistence length (6) $\xi_p \equiv a \exp(c\kappa/kT)$,
where a is a short-distance cutoff and $c =$
 $4\pi/3$ (7, 8). However, as L approaches ξ_p ,
shape fluctuations have been predicted (7, 8)
to reduce the bending rigidity and lead to a
renormalized rigidity $\kappa_R = \kappa - (kT/c)$
 $\ln(L/a)$ in the limit of small kT/κ . On length
scales $L \approx \xi_p$, the membrane should have an
effective bending rigidity of the order of kT .
At larger length scales ($L \gg \xi_p$), mem-
branes fluctuating at constant area are ex-
pected to have an extremely small bending
rigidity and behave as crumpled (9) objects
characterized by the absence of long-range
orientational order of normals erected per-
pendicular to the local surface elements. For
a fixed topology, the scaling behavior of
self-avoiding fluid membranes at these
length scales is expected to be the same as
that of a branched polymer (2, 10, 11).

Several aspects of this scenario have, how-
ever, not yet been verified. Indeed, there is
little evidence that self-avoiding fluid mem-
branes with a finite bare bending rigidity
really do crumple. It has been speculated (2)
that self-avoidance may stabilize the effective
bending rigidity at some finite value $\kappa \sim kT$
and therefore prevent crumpling. Further-
more, there is some controversy concerning
the universality classes of the various models
used to describe self-avoiding random sur-
faces (with $\kappa = 0$). The most widely studied
models for these surfaces are constructed by
taking the elementary 2-cells (plaquettes) on
a hypercubic lattice and gluing them togeth-
er in such a way that each edge is shared by
exactly two plaquettes (10). For fixed topol-
ogy, the long-length-scale behavior of this
class of surface has been shown to be that of
a branched polymer: the radius of gyration
 R_g of a surface of area S scales as $R_g^2 \sim S^{\nu}$
(12), with $\nu = 1$ in spatial dimension $d = 3$
(10). Recently, however, randomly triangu-
lated surfaces of the type we consider here
have been investigated for $\kappa = 0$ with the
use of Monte Carlo techniques (13). A value
 $\nu \approx 0.8$ was reported, implying that such
surfaces belong to a different universality
class. Given the generality of the entropic
mechanism behind branched polymer be-
havior, this discrepancy is troubling (10,
11).

In this report we present evidence that
fluid membranes are crumpled at sufficiently
large length scales for any value of the bare
bending rigidity and that the crumpled state
does indeed exhibit branched polymer be-
havior. Our conclusions are based on exten-

D. M. Kroll, AHPARC, University of Minnesota, Min-
neapolis, MN 55415.

G. Gompper, Sektion Physik der Ludwig-Maximilians-
Universität München, 8000 München 2, Germany.

*Permanent address: Institut für Festkörperforschung,
KFA Jülich, 5170 Jülich, Germany.

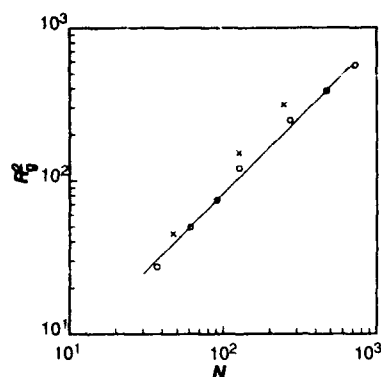


Fig. 1. Mean-squared radius of gyration R_g^2 versus the number of monomers N for $\lambda = 0$: (○) open membrane, $\ell_0^2 = 2.0$, free-edge boundary condition; and (×) vesicle, $\ell_0^2 = 2.8$. The solid line is a plot of $R_g^2 \sim N$.

sive simulations of a simple molecular model for self-avoiding fluid membranes for a wide range of bare bending rigidities. The simulations were carried out with a simple string-and-bead model for randomly triangulated two-dimensional surfaces embedded in three dimensions (13–17). Both planar (with free-edge boundary conditions) and spherical (vesicle) topologies were considered. In both cases the surface is modeled by a triangular network of N hard-sphere particles of diameter $\sigma = 1$. The energy assigned to a particular configuration is

$$\beta\mathcal{H} = -\lambda \sum_{\langle\alpha,\gamma\rangle} (\mathbf{n}_\alpha \cdot \mathbf{n}_\gamma - 1) + \sum_{\langle i,j \rangle} V_t(|\mathbf{r}_i - \mathbf{r}_j|) + \sum_{i>j} V_{HC}(|\mathbf{r}_i - \mathbf{r}_j|) \quad (1)$$

where $\beta = 1/kT$. In Eq. 1, the first sum runs over pairs $\langle\alpha,\gamma\rangle$ of unit vectors $\{\mathbf{n}_\alpha\}$ erected perpendicular to each elementary triangle in the lattice. The second summation is over neighboring pairs $\langle i,j \rangle$ of atoms (located at \mathbf{r}_i and \mathbf{r}_j) in the array interacting through a tethering potential $V_t(r)$ that vanishes for $0 < r < \ell_0$ and is infinite otherwise. Finally, the third summation is over all pairs of atoms interacting through a repulsive hard core potential $V_{HC}(r)$ that vanishes for $r > 1$ and is infinite otherwise. Self-avoidance is enforced by choosing an $\ell_0 < \ell_0^{\max}$; the value of ℓ_0^{\max} depends on the updating procedure that is implemented (see below). The continuum limit of the bending energy term in Eq. 1 can be shown to be

$$F_b = \frac{1}{2} \kappa \int dS (H^2 - 2K) \quad (2)$$

where dS denotes the surface element and F_b is just Helfrich's curvature elastic energy with bending rigidity $\kappa = \lambda/\sqrt{3}$ (18, 19) and Gaussian rigidity $\kappa_G = -\kappa$; $H = c_1 + c_2$ and $K = c_1 c_2$, where c_1 and c_2 are the principal curvatures.

Our Monte Carlo updating procedure consists of two steps: First, we attempt to sequentially update the position vector of each monomer by a random increment in the cube $[-s, s]^3$, where s is a constant to be chosen below. The probabilistic decision whether to accept the move is made by comparing the initial and final energies of the system. We chose s so that $\sim 50\%$ of the updating attempts were accepted. Second, we attempt to flip N randomly chosen bonds. A bond flip consists of deleting a tether and constructing a new one between the two previously unconnected vertices of the two adjacent triangles. The flip is accepted with the probability given by the Boltzmann factor if all vertices have a minimum of three neighbors (20). Note that this procedure does not flip boundary tethers, so that the open membranes we simulate have perimeters of constant length. A more detailed discussion of the bond-flipping procedure can be found in (13–17).

In order to insure reparametrization invariance we use a discretized version of the invariant measure $\int D[\mathbf{r}] = \prod_\xi [d\mathbf{r}(\xi) g^{3/4}(\xi)]$ in our simulations, where $\mathbf{r}(\xi)$ is the three-dimensional coordinate vector of a point on the surface with internal coordinate ξ and g is determinant of the metric tensor (21). We also choose a metric in which all internal lengths are equal, that is, all triangles on the surface are equilateral and of area one so that the volume ω_i of the dual image of vertex i (which is the discrete analog of the invariant volume $\int d^2\xi \sqrt{g}$) is proportional to the coordination number q_i of this vertex: $\omega_i = q_i/3$. On the triangulated surface the curvature is concentrated at the vertices; with the present normalization the scalar curvature $R_i = \pi(6 - q_i)/q_i$, and the discretization of the measure is $\prod_i d\mathbf{r}_i \omega_i^{3/2}$ (14–17).

Simulations were performed with both ℓ_0

$= \sqrt{2.0}$ and $\sqrt{2.8}$. In the former case we chose $s = 0.1$ and in the latter $s = 0.15$. This choice of parameters ensures self-avoidance when updating the monomer coordinates. However, there is only weak self-avoidance during bond flipping for $\ell_0 = \sqrt{2.8}$. Indeed, it is easy to show that implementing complete self-avoidance would require taking ℓ_0 at least less than $\sqrt{8/3}$ in this case. We have in fact observed vesicle inversion for $\ell_0 = \sqrt{2.8}$ when $\lambda = 0$. Nevertheless, data for the mean-squared radius of gyration R_g^2 for zero bending energy indicate that this does not influence the asymptotic fractal dimension of the crumpled phase. Furthermore, it does not qualitatively affect the behavior for finite λ . The primary advantage of using a larger tethering length is that the diffusivity of the monomers in the membrane surface is substantially enhanced: the bond-flip acceptance rate is a factor of 2 greater for $\ell_0 = \sqrt{2.8}$ than for $\sqrt{2.0}$ when $\lambda = 0$; the effect is greater for larger values of λ .

In Fig. 1 we plot data for R_g^2 versus the number of monomers for the case of zero bending rigidity, $\lambda = 0$. Averages were taken over 1×10^7 to 2×10^7 Monte Carlo steps per monomer. Data are shown both for vesicles with $\ell_0 = \sqrt{2.8}$ and planar membranes with $\ell_0 = \sqrt{2.0}$. For both topologies, the data are consistent with $R_g^2 \sim N^\nu$ (12) with $\nu = 1$. Furthermore, typical configurations, such as the one illustrated in Fig. 2, indicate a "branched polymer" structure in which there are long arms extending out in various directions. This result suggests an entropic mechanism that favors treelike ramified objects, which is in agreement with results obtained for random surfaces constructed of elementary plaquettes on a cubic lattice (10). For vesicles, our results are consistent with $S \sim R_g^2$ and $V \sim R_g^2$ (where S and V are the surface area and

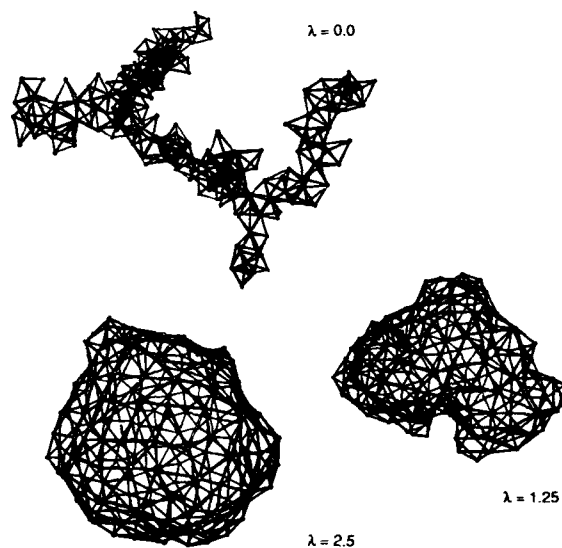


Fig. 2. Typical configurations of a vesicle with $N = 247$ monomers and $\ell_0 = \sqrt{2.8}$ for $\lambda = 0, 1.25$, and 2.5 .

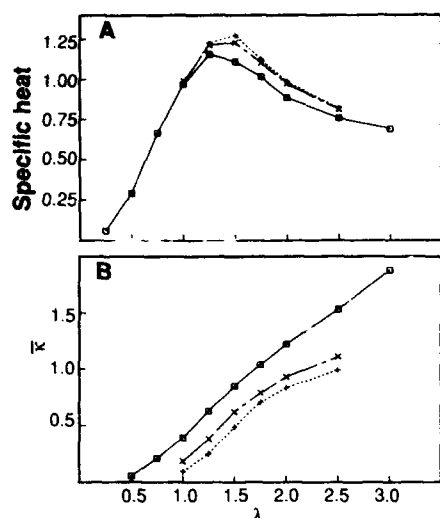


Fig. 3. (A) Specific heat obtained by using Eq. 3 for vesicles with $\ell_0 = \sqrt{2.8}$ and $N = (\square)$ 47, (\times) 127, and $(+)$ 247 monomers. (B) Effective bending rigidity $\bar{\kappa} = \kappa_{\text{eff}}/6$ obtained by averaging over $N_s = (N - 1)/2$ contiguous monomers on the vesicle surface by using Eq. 5.

volume enclosed by the vesicle).

Fluctuations are suppressed for finite λ , and as seen in Fig. 2, there appears to be a crossover from crumpled behavior for $\lambda \ll 1$ to a rough but extended phase for $\lambda \gg 1$. Further evidence for this freezing out of degrees of freedom is given by the behavior of the specific heat per monomer

$$C \equiv \frac{\lambda^2}{N} [\langle E^2 \rangle - \langle E \rangle^2] \quad (3)$$

where $E = \sum_{\alpha, \beta} \mathbf{n}_\alpha \cdot \mathbf{n}_\beta$. A plot of data obtained for vesicles with $\ell_0 = \sqrt{2.8}$ containing $N = 47$, 127, and 247 monomers (Fig. 3A) shows that there is a pronounced peak near $\lambda_c \approx 1.25$. Such a peak could signal the existence of a phase transition between a crumpled phase for low bending rigidities and a flat phase for large ones. In fact, it is argued in (17) that such a transition does indeed occur in membranes without self-avoidance. However, the height of the peak increases only slowly with N . This result implies that the specific heat exponent α must be very small (if there is a transition) or that the correlation length exponent ν must be quite large. In addition, the peak shifts to larger values of λ with increasing system size, which is the opposite of what is usually observed for finite size effects in systems with periodic boundary conditions. We believe the most plausible explanation is that the peak occurs when the persistence length ξ_p reaches the system size and that there is no phase transition.

An additional confirmation of this interpretation is given by the behavior of the scale-dependent effective bending rigidity

κ_{eff} . The renormalized bending rigidity can be expressed in terms of the mean curvature susceptibility as (22)

$$\langle A \rangle / \kappa_{\text{eff}} = \int d^2 \xi \sqrt{g(\xi)} \int d^2 \xi' \sqrt{g(\xi')} \langle H(\xi) H(\xi') \rangle_c \quad (4)$$

where $\langle A \rangle$ is the average membrane area, $\langle \dots \rangle_c$ denotes the cumulant average, and $H(\xi)$ is the mean curvature at ξ . In the continuum limit, the extrinsic curvature tensor is proportional to the unit normal vector. The discretization (23) of $\int d^2 \xi \sqrt{g(\xi)} H(\xi)$ we use is therefore $\sum_i s_i |\sum_{j(i)} (\sigma_{ij}/l_{ij})(\mathbf{r}_i - \mathbf{r}_j)|$, where the i -sum runs over monomers, the $j(i)$ -sum runs over the neighbors of i , and s_i is the sign of $\hat{\mathbf{n}}_i \cdot \sum_{j(i)} (\mathbf{r}_i - \mathbf{r}_j)$, with $\hat{\mathbf{n}}_i$ the surface normal at monomer i obtained by averaging over the normals of all triangles that have i as a corner; l_{ij} is the distance between the two neighboring monomers i , j , and σ_{ij} is the length of a bond in the dual lattice. For the metric we have chosen, $\sigma_{ij}/l_{ij} = 1/\sqrt{3}$ so that the right-hand side of Eq. 4 becomes

$$\frac{1}{3} \langle \sum_i s_i |\sum_{j(i)} (\mathbf{r}_i - \mathbf{r}_j)| \sum_k s_k |\sum_{m(k)} (\mathbf{r}_k - \mathbf{r}_m)| \rangle_c \quad (5)$$

For vesicles, the amplitude of the average in Eq. 4 depends strongly on the size of the region over which one averages. In particular, in the continuum limit, one finds that $\kappa_{\text{eff}} = 6\kappa$ when averaging over one-half of a sphere when fluctuations are ignored. Our results for $\bar{\kappa} = \kappa_{\text{eff}}/6$, obtained by averaging over $N_s = (N - 1)/2$ contiguous sites on the vesicle surface, are shown in Fig. 3B (24); κ_{eff} is a decreasing function of N for all λ . There does not appear to be any qualitative difference in the behavior of κ_{eff} for large and small λ .

We have not attempted to make a quantitative comparison with theory in the large λ regime, because the expected logarithmic renormalization of κ is completely masked by averaging over a finite portion of the membrane surface (25). Nevertheless, the essential qualitative feature that κ_{eff} is a decreasing function of length scale in both the large and small λ regimes supports the interpretation that there is no phase transition as a function of λ .

Self-avoiding fluid membranes are therefore very likely always crumpled at large length scales, independent of the value of the microscopic bending rigidity κ . Furthermore, the crumpled state of the model we considered is a treelike ramified object characterized by $R_g^2 \sim N$, in agreement with results obtained for hypercubic plaquette models (10) of random surfaces. A more detailed analysis, however, is required to

determine the quantitative scale dependence of the renormalized bending rigidity.

Fluid membranes with a wide range of bare bending rigidities have been studied experimentally in considerable detail recently. For phospholipid bilayers at room temperature, $\kappa/kT \approx 10$ to 20 [see (26–28), which contain many additional references], so that the persistence length is usually much greater than the size of the membranes and the reduction of the bending rigidity by shape fluctuations is negligible. An exceptionally small value for ξ_p , however, is obtained for lecithin membranes containing a small amount of bipolar lipid (26); this may also be the case for surfactant bilayers that form lamellar and bicontinuous phases (29). These systems are therefore well suited for experimental studies of flexible fluid membranes.

We have shown that simulations performed using simple string-and-bead models for randomly triangulated surfaces (with a wide range of finite bare bending rigidities) can yield detailed information on both the large-length-scale conformation as well as the scale dependence of elastic constants such as the bending rigidity. Further numerical studies of this model and its generalizations should permit a more detailed comparison with experiment and could provide new insight into many phenomena involving membranes and other self-assembling structures.

REFERENCES AND NOTES

1. D. R. Nelson, T. Piran, S. Weinberg, Eds., *Statistical Mechanics of Membranes and Surfaces*, (World Scientific, Singapore, 1989).
2. R. Lipowsky, *Nature* **349**, 475 (1991).
3. The precise definition of the lateral tension in fluctuating membranes is a somewhat subtle and often confused issue. See (4) for a discussion of this point.
4. F. David and S. Leibler, *J. Phys. II France* **1**, 959 (1991).
5. F. Brochard and J. F. Lennon, *J. Phys. (Paris)* **36**, 1035 (1975).
6. P. G. de Gennes and C. Taupin, *J. Chem. Phys.* **86**, 2294 (1982).
7. L. Peliti and S. Leibler, *Phys. Rev. Lett.* **54**, 1690 (1985).
8. D. Forster, *Phys. Lett.* **114A**, 115 (1986); H. Kleinert, *ibid.*, p. 263; *ibid.* **116A**, 57 (1986).
9. We follow the current general usage of the word crumpled to describe a fractal, self-similar object for which all eigenvalues of the moment-of-inertia tensor scale with the same exponent.
10. U. Glaes, *Phys. Rev. Lett.* **56**, 1996 (1986); *J. Stat. Phys.* **50**, 1141 (1988).
11. M. E. Cates, *Phys. Lett.* **161B**, 363 (1985).
12. This definition of ν corresponds to that generally used in studies of tethered membranes. It has also been used in (2) and (13) to describe the crumpled state of fluid membranes. This definition of ν is twice that used in (10).
13. J.-S. Ho and A. Baumgärtner, *Europhys. Lett.* **12**, 295 (1990); A. Baumgärtner and J.-S. Ho, *Phys. Rev. A* **41**, 5747 (1990).
14. J. Ambjörn, B. Duurhuus, J. Fröhlich, *Nucl. Phys. B* **257**, 433 (1985); *ibid.* **275**, 161 (1986).
15. D. V. Boulatov, V. A. Kazakov, I. K. Kostov, A. A. Migdal, *ibid.*, p. 641.
16. A. Billoire and F. David, *ibid.*, p. 617.

17. C. F. Baillie, D. A. Johnston, R. D. Williams, *ibid.* **335**, 469 (1990).
18. This result can be obtained by covering a sphere with equilateral triangles of side ℓ and taking the limit $\ell \rightarrow 0$. A similar procedure was followed in (19) for a cylindrical surface; in that case it was found that $\kappa = \sqrt{3}\lambda/2$.
19. H. S. Seung and D. R. Nelson, *Phys. Rev. A* **38**, 1005 (1988).
20. Unlike (13) (in which the maximum number of nearest-neighbor bonds was limited to eight), we do not explicitly restrict the maximum number of neighbors. We find, for example, that the average maximum connectivity of a monomer is ~ 12 for the largest systems studied (for $\lambda = 0$). We have checked, however, that restricting the maximum number of nearest neighbors as in (13) does not prevent the observed collapse to branched polymer behavior.
21. K. Fujikawa, *Nucl. Phys. B* **226**, 437 (1985).
22. G. Gompper and D. M. Kroll, *J. Phys. I France* **1**, 1411 (1991).
23. C. Itzykson, in *Proceedings of the GIFT Seminar, Jussieu*, J. Abad *et al.*, Eds. (World Scientific, Singapore, 1986), pp. 130–188.
24. In evaluating $\bar{\kappa}$ we have used $\langle A \rangle = 2N_e(1 - 2/N_e)$ (A_Δ), with $\langle A_\Delta \rangle \approx 0.78$, where $\langle A_\Delta \rangle$ is the average area of an elementary triangle.
25. See (22) for a partial treatment of this problem for tethered membranes.
26. H. P. Duwe, J. Käs, E. Sackmann, *J. Phys. (Paris)* **51**, 945 (1990).
27. E. Evans and W. Rawicz, *Phys. Rev. Lett.* **64**, 2094 (1990).
28. M. Mutz and W. Helfrich, *J. Phys. (Paris)* **51**, 991 (1990).
29. J. M. Di Miglio, M. Dvolaitzky, L. Leger, C. Taupin, *Phys. Rev. Lett.* **54**, 1686 (1985).
30. Supported in part by the University of Minnesota Army High Performance Computing Research Center, U.S. Army contract DAAI.03-89-C-0038, NATO grant CRG910156, and the Deutsche Forschungsgemeinschaft through Sonderforschungsbereich 266. D.M.K. has benefited from correspondence with M. E. Fisher and discussions with G. Grest.

30 September 1991; accepted 24 December 1991